BNAM2012
Joint Baltic-Nordic Acoustics Meeting
June 18th - 20th 2012 Odense, Denmark

Detection of pit clusters in pipes using the fundamental torsional guided wave

Anders Løvstad
Multiconsult AS, Postboks 265 Skøyen, N-0213 Oslo, Norway, anders.lovstad@multiconsult.no

Presently, the offshore petroleum industry moves their operational activities to harsher environments, leading to increased risk and occurrence of corrosion. A guided wave technique using the fundamental torsional guided wave is applied in order to assess and evaluate the detectability of pitting corrosion in steel pipes. A parametric study of part- and through thickness holes that are small compared to the wavelength of the interrogating signal is discussed first, before the reflection from pit clusters with a random number of holes of random size and depth are evaluated using the finite element method. For realistic pit cluster morphologies, good detectability was found.

1 Introduction

Corrosion of carbon and low-alloy steels, which are used extensively in the petro-chemical industry, is a major concern for the integrity of subsea pipelines as the offshore petroleum industry moves its operational activities to harsher environments, with higher pressure and temperatures, deeper depths, and multi-phase transportation through subsea completions, all of which increase the risk of corrosion [1]. The morphology of corrosion attack ranges from general corrosion, where the entire surface is evenly attacked, to localised corrosion which is limited to discrete sites, such as pitting and pit clusters, mesa corrosion and crevice corrosion. Pits can be of various shapes and sizes, grow together to form larger pits, and/or develop adjacent to each other to form pit clusters. When leaks, ruptures or fatigue occur in pipelines it is usually caused by internal H_2S/CO_2 corrosion resulting from large, wide pits and pit clusters [2].

The corrosion rate and growth law of localised corrosion is very variable, as is the maximum pit depth compared to the mean wall loss [3]. However, after longer exposure times, when pits are measured in millimetres rather than micrometres, their growth develops differently from the initial stages of development. Both Melchers [4] and Engelhart et al [5] reported that corrosion pits tend to grow faster in width than in depth as they increase in size. With pit clusters, the maximum pit depth may change between different pits as the clusters develop with time, and commonly there are several pits that have reached a given depth within the cluster [4].

In employing the guided waves non-destructive testing (NDT) technique, the fundamental torsional mode, T(0,1), is most commonly used for practical inspection in pipes. Many researchers have investigated the scattering and reflection from a variety of defects using guided waves in pipes [6, 7]. The aims of ultrasonic guided wave testing are to detect and size defects, and especially to quantify the maximum depth of defects within the area inspected to evaluate whether they will lead to structure failure. Long range screening of pipelines using cylindrical guided waves typically aims to detect defects of order 5% or more of the cross-sectional area at a given axial distance [7], but defects down to 1% of cross-sectional area can be detected under optimal testing conditions. Long range guided wave testing generally uses frequencies below 100 kHz, with bandwidths of around 30-50 kHz.

This paper initially reports on the reflection from two small circular holes in a pipe. As localized corrosion often occurs in clusters, the understanding of the reflection from two circular holes at different relative orientations will be a step towards understanding the scattering behaviour of multiple and randomly spaced defects. The validity of employing the superposition technique in calculating the reflection coefficients (RCs) is assessed, the results of which forms the basis for an investigation of the reflection from randomly generated pit clusters.

2 The reflection from two small circular holes

2.1 Method and finite element modelling

Full 3D models in the commercially available software Abaqus are employed to model the various defect layouts investigated, modelling a 3 meter long, 3 in. schedule 40 pipe. A 4 cycle Hanning windowed toneburst with centre frequency of 60 kHz was used, giving a ±10 dB bandwidth of roughly 40-80 kHz. The model was validated against the analytical solution [8, 10] in the single hole case.

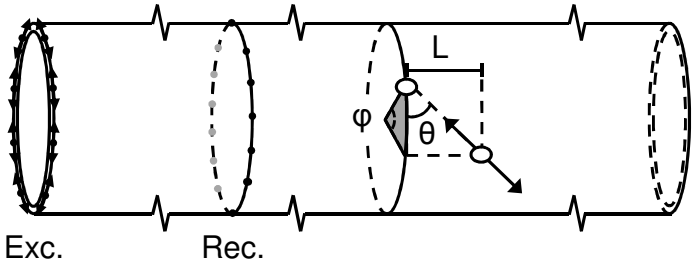

Figure 1: Schematic of defect layouts of circular holes separated circumferentially ($L = 0$), axially ($\varphi = 0$), and at intermediate positions.

Defect layouts were modelled as shown in Figure 1 for defects separated circumferentially ($L = 0$), axially ($\varphi = 0$), and at other relative positions. The arrow indicates the way in which defect separation was varied. Most of the simulations were compared with results obtained using the superposition principle, where separate simulations were performed with one defect at a time, the reflected signals being subsequently added together directly, thus also evaluating the uncertainty in the numerical predictions. Using the superposition approach implicitly neglects interaction between the defects.

The T(0,1) mode was excited by applying the excitation toneburst as tangential displacements at evenly spaced nodes around the outer circumference at one end of the pipe, as indicated in Figure 1. Similarly, 90 monitoring points were used as receivers. The pipe length, location of receiver positions and defect location were chosen so that the incident and reflected signals could be well separated. Reflection coefficients were calculated in the frequency domain as the ratio of the surface circumferential displacement amplitude of the reflection to the incident amplitude.

2.2 Results

Only results for the T(0,1) at the toneburst centre frequency of 60 kHz will be discussed here. A more elaborate discussion, including results within the full ±10 dB bandwidth of the interrogating signal, the reflection of mode converted modes, and results with three holes, is given in [10]. Figure 2 (a) shows RCs for the T(0,1) mode at 60 kHz as a function of the angular distance φ between the holes for a single circular hole (I) and two circumferentially spaced through-thickness circular holes (II), as well as for two circumferentially spaced holes of 50% depth (III), all of diameter $d = t$. The minimum angle between defects modelled is $\varphi = 11°$, corresponding to a minimum separation distance of $1.15d$; smaller separation between them would lead to highly distorted meshes, and result in numerical problems. RCs for the full solution are shown in solid lines, while superposition results are shown in dashed lines.

The RC for a single (I) circular through-thickness hole is approximately 2.5%, which roughly doubles to 5% with two (II) through-thickness holes for all angular separations. The RC is relatively independent of the circumferential position of the holes, except when the angular separation is below 20°, which corresponds to an angular separation of two diameters centre to centre. The deviation between the full solution and superposition is due to multiple scattering between the defects.

The RC for two circumferentially spaced defects of 50% depth is shown in (III), where the rise in RC due to multiple scattering and interaction between the holes at small φ can be seen to be far less than for through-thickness holes, indicating a wider validity of the superposition approach for part-thickness defects. Also, the oscillation about the superposition results seen for through-thickness defects is not present to the same extent, due to reduced multiple scattering from part-depth holes. Excellent agreement is seen between RCs with both defects present and superposition for defects of 50% depth.

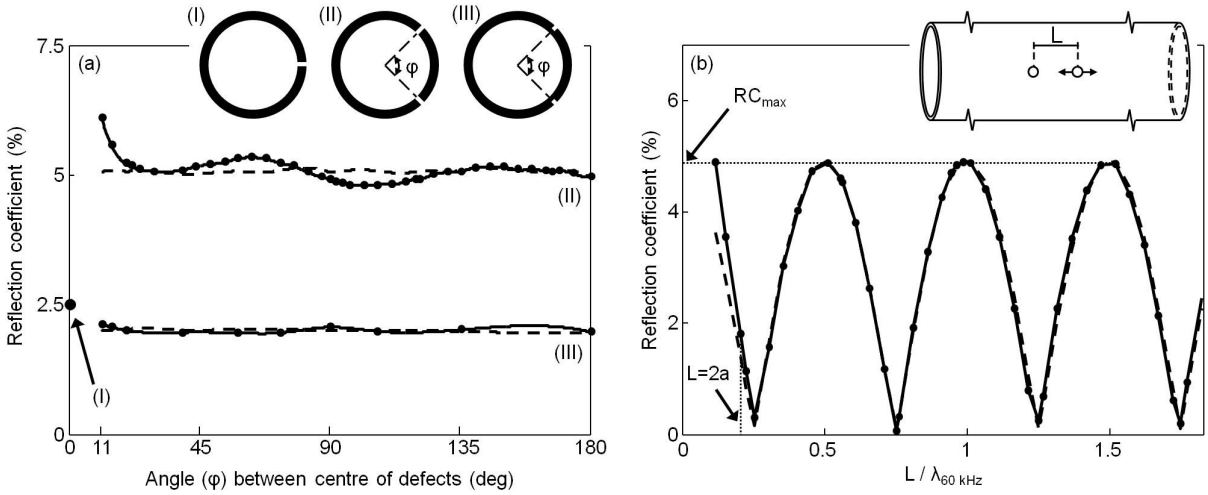

Figure 2: Variation of reflection coefficient at 60 kHz with (a) angle between circumferentially spaced circular holes of diameter $d = t$, (b) axial separation for two through-thickness circular holes of diameter $d = t$.

With axially spaced defects, reflections will arrive at different times, giving rise to interference effects. Figure 2 (b) shows the RC at 60 kHz as a function of the ratio L / λ_{60k}, where L is the separation distance from centre to centre of the two circular holes, as shown in the figure inset. The RC can be seen to be strongly dependent on L, maxima occurring at $L\eta / (2\lambda)$, where η is an integer. Excellent agreement is found between simulations with the full solution (solid line) and superposition (dashed line), with increasing deviation for $L < 2d$. The maximum RC is around 5%, which is comparable to that for circumferentially spaced defects.

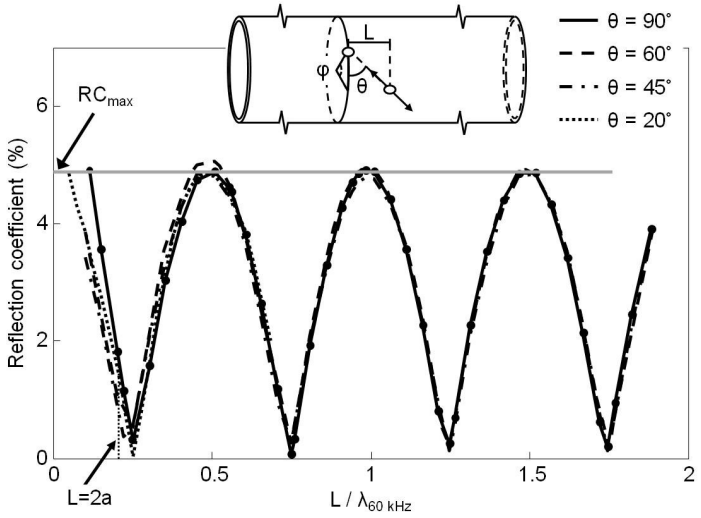

Figure 3: Variation of the T(0,1) reflection coefficient with axial separation for two through-thickness circular holes of diameter $d = t$ at $\theta = 20$, 45, 60 and 90°.

Figure 3 shows the RC at 60 kHz from two circular through-thickness holes as a function of the ratio of the axial separation distance to the wavelength at different relative orientations given by the angle θ, as shown in the figure inset. Calculations were done for $\theta = 20$, 45, 60 and 90°, shown in dotted, dash-dotted, dashed and solid lines, respectively. All the RCs display the same interference behaviour, with maxima of approximately 5% (as for the circumferentially separated defects discussed above, as indicated by the grey line) at multiples of $L\eta / (2\lambda)$, indicating that the RCs are independent of the circumferential position of the defects for $L > 2d$. At $L < 2d$, multiple scattering increasingly influences the RC.

3 The reflection from pit clusters

For single defects successive peaks in the RC occur at $L/\lambda = \eta/4$, while the RC is linearly proportional to the circumferential extent of the defect [6, 7, 10]. With two axially separated holes, successive peaks occur at $L/\lambda = \eta/2$, regardless of their circumferential position, as seen in Section 2.2. As the corrosion attacks become more complex, possibly consisting of multiple defects of various depth, size and shapes, RCs become complex, frequently consisting of multiple peaks. In practical test situations the number and shape of defects are unknown, and the frequency range employed in the test will be limited by the testing equipment. Most commonly the maximum RC is used as the evaluation parameter, which is a sensible choice as the possible presence and values of peaks in the RC within the bandwidth of the interrogating signal depend on the geometrical properties of the defect(s).

As mentioned earlier, the maximum defect depth within the testing range is the most important parameter to quantify in most NDT. Following the discussion in the previous section, estimation of RCs from pit clusters consisting of a random number of pits that have developed randomly in size and depth following certain growth rules is considered.

3.1 Method and finite element modelling

As in Section 2, full 3D FE models were employed throughout, in this case with 4 in. nominal bore schedule 40 pipes. A 2 cycle Hanning windowed toneburst with centre frequency of 50 kHz was used to excite the T(0,1) mode, similarly as explained above. The pipe length, location of receiver positions and defect location were chosen so that the incident and reflected signals could be well separated as Figure 4 (a) shows, exemplified by a defect grid with both axial and circumferential size equal to a quarter of the pipe circumference, $d_{ax} = d_{circ} = 2\pi r_{pipe}/4$. The term grid designates possible pit initiation sites as shown in Figure 4 (b), while the term mesh is used in relation to the FE resolution. RCs were calculated as explained above, and convergence tests were run to ensure appropriate mesh size and time steps.

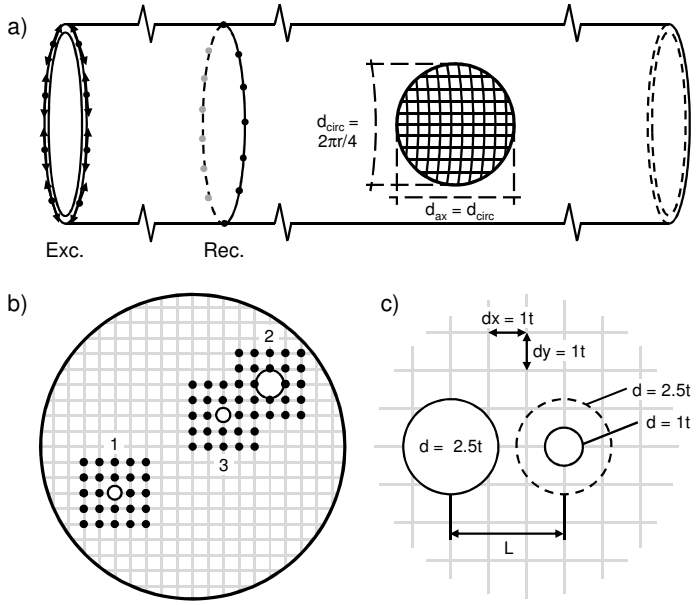

Figure 4: (a) Schematic of finite element models and cluster grid. (b) Random selection and spacing requirement between adjacent pit locations. (c) Details of grid size and minimum separation between adjacent pits; thus $L \geq 1.2d$ with a grid size of $1t$.

A simplistic model for the cluster development is used, where the clusters develop through a random number of development steps. For each step there is equal probability at which grid node within the defect grid a pit will grow. If a pit is already present at the given grid node, the pit will grow either in depth or in width with equal probability. Flat-bottomed circular holes are used, with defect diameters from $1t$ to $2.5t$ in increments of $0.25t$, and with increments in depth of 10% of the pipe wall thickness. If a pit has reached maximum depth it may only grow in width, and vice versa. If the maximum width and depth have been reached, the grid point is unavailable for selection. The reason for limiting the maximum pit diameter to $2.5t$ is related to the use of superposition.

Figure 4 (b) shows an example cluster grid with three defects at the given stage of development. The black dots around the holes indicate grid nodes where no new pit can be initiated once the three holes shown are present, to keep pits from growing into each other; if any of these intermediate nodes is selected, the choice is ignored and a reselection is made. A grid size of $dx = dy = 1t$ was chosen and employed throughout the simulations, as shown in Figure 4 (c). With the largest pit size of diameter $d = 2.5t$ and a grid size of $1t$, the lowest separation possible between pits then becomes $L = 1.2d$ centre to centre, for which acceptable validity of employing superposition is achieved, as discussed below. This situation is shown in Figure 4 (c), which shows a $d = 2.5t$ pit to the left, and the closest a new pit may initiate to the right, where the initial ($d = 1t$) and maximum ($d = 2.5t$) pit sizes are indicated by solid and dashed circles, respectively. With this grid size, range of pit sizes in width and depth, and a circular defect domain in which pits can grow of size $d_{ax} = d_{circ} = 2\pi r_{pipe}/4$, the lowest number of growth steps that can leave no valid growth step remaining is 126. Thus, a random number of pit development steps in the range 1-126 was employed.

To be able to evaluate large numbers of randomly developed pit clusters, the superposition technique is employed to calculate the RCs. Superposition is valid if $L \geq 2d$ in the worst case with through-thickness defects, as seen in Section 2.2 and in similar studies for bulk waves [11]. However, for part-thickness defects, the validity was found to be significantly better [10]. Obviously, with less developed pit clusters consisting of coarsely populated clusters and/or pits of small diameter, centre to centre distances between pits are likely to be larger than the worst case of $L = 1.2d$. Superposition calculations are based on FE calculations of single defect types; each defect type (i.e. possible pit sizes and diameters) was simulated using the model shown in Figure 4 (a). Based on the location and type of pits in the randomly generated pit clusters, the appropriate time delay (or phase delay in the frequency domain) was added to the reflection from each pit in the cluster depending on their position. Finally, all the shifted reflections from the defects were added together to obtain the total pit cluster reflection, and the total RC of the cluster was calculated as the ratio of the sum of all the reflections from the individual defects to that of the incident signal.

Extensive comparison between full solution and superposition results was done, as reported in [12]. Clearly, the finer the defect grid used, the larger number of possible initiation sites for pits in the clusters, which is desirable in order to model as realistic cluster layouts as possible. With the grid size used here a deviation between the full solution and superposition in maximum RC less than 4% in most cases, and the maxima occurred at frequencies within 5% of each other. With highly developed clusters, where several large and deep pits were adjacent to each other, a somewhat larger shift in frequency was seen in some cases, but the deviation in maximum RC was within 10% in all cases.

3.2 Results

Figure 5 (a) shows the maximum RC as a function of defect volume fraction for 2000 example layout cases, where frequencies up to 75 kHz are included in the analyses. The defect volume fraction is given by the ratio of total pit volume to the volume of the circular defect domain multiplied by the pipe wall thickness. As expected, the maximum RC follows a linear trend with increasing volume removed from the pipe (more developed clusters), with very significant scatter due to the axial extent of the clusters, as reflections from discrete pits may interfere destructively, leading to lower maximum RCs.

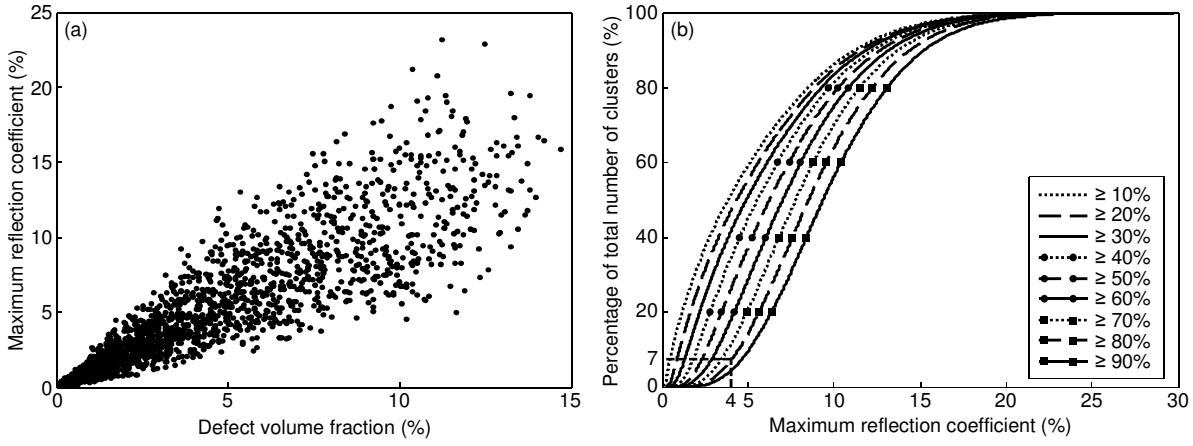

Figure 5: (a) Maximum RC as a function of defect volume fraction. (b) Percentage of clusters with a maximum RC less than the values of the abscissa for maximum pit depths greater than the thresholds indicated in the legend.

The sample results shown in Figure 5 (a) illustrate the usefulness of applying a statistical approach in the evaluation of possible pit clusters and other complex corrosion patches in determining probable maximum RC ranges and distributions. Here we will be interested in the percentage of pit clusters in which there is a pit with maximum depth larger than a given value that give maximum RCs that are less than given values, and would therefore be difficult to detect. Figure 5 (b) shows the percentage of clusters with maximum RC less than the values of the abscissa for maximum pit depths deeper than given depth values, as indicated in the figure legend. The maximum RCs and depth percentages are calculated from a series of 100,000 randomly generated pit clusters. The example value for interpretation indicated by the dashed line in Figure 5 (b) indicates that in 7% of the cases with pit clusters with maximum depth deeper than 80% the maximum RC is less than 4%.

Cluster morphologies with low maximum RC and deep maximum depth are problematic from a NDT detection point of view. Most of the pit clusters with large maximum cluster depth and low maximum RC result from layouts that consist of many pits, of which most are quite shallow and/or small, with one small, deep pit. Such single, small through-thickness pits are improbable from a practical corrosion morphology point of view [4, 5], which is encouraging for practical guided wave testing, as isolated pits are very difficult to detect. However, in some cases pit clusters consisting of several rather deep pits (in addition to some shallower ones) also result in low maximum RCs due to destructive interference between pits in the cluster, as well as the limited bandwidth inherent in practical guided wave testing.

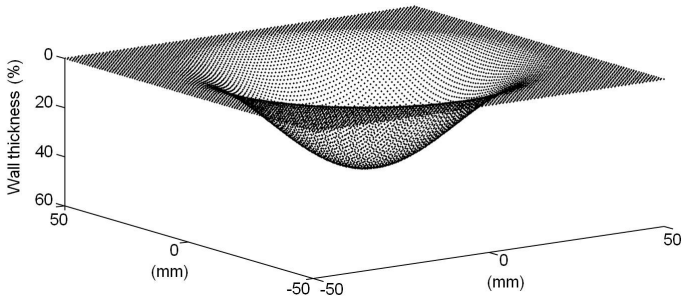

Figure 6: Example 40% deep cosine taper, shown unwrapped onto a plate.

So far all pit clusters are based on flat bottomed circular pits growing out of areas affected by general corrosion only. However, pits are likely to be part of a larger, broader attack [2], and are thus surrounded by areas of significant wall loss in which the pits are the deepest parts, especially for mild and low-alloy and carbon steels [4]. To accommodate this feature, the pit clusters were superposed on a circular cosine tapered defect with diameter $2\pi r_{pipe}/4$. Figure 6 shows an example cosine taper of depth 40% of the wall thickness. The geometry is shown straightened out onto a plate for clarity, but all simulations were done on the same 4 in. schedule 40 pipe as in shown in Figure 4 (a). The RCs from such cosine tapers scale approximately linearly with defect depth, with the maximum RC occurring around 18 kHz, at which the cosine taper size $d_{ax} = 2\pi r_{pipe}/4$ corresponds to $\lambda/4$ for the T(0,1) mode. This is in accordance with earlier studies of single defects [6, 7]. At such low frequencies, the interrogating signal will not see the pits separately, but as parts of the larger cosine taper defect, which increases the low frequency RC.

To be able to run a large number of random clusters, use of superposition is a necessity. In applying superposition with a cosine taper, it is assumed that the RC from each pit is proportional to the volume removed, from which it follows that the mode shape of the T(0,1) mode is constant through the pipe wall thickness, and all pits give the same reflection regardless of their position through the thickness of the pipe. Additionally, the pits will not fit perfectly onto the cosine taper as they are simply shifted down onto the cosine taper using the centre point of each pit. As they are flat-bottomed, an error inferred, the severity of which depends on the gradient of the cosine taper at the specific location. Both these approximations are inherently accepted in the superposition calculations. A thorough discussion of the validity of applying the superposition approach is included [12], which concludes that the main features of the RC are obtained, and most importantly both the local and global maxima show good agreement, validating the use of superposition with cosine tapers within acceptable accuracy.

Percentages of clusters with maximum depth exceeding certain thresholds as a function of maximum RC were calculated for pit clusters with various depths of the underlying cosine taper. Figure 7 shows results for pit clusters with maximum RC less than the values of the figure abscissa for clusters with maximum defect depth deeper than, or equal to, 60% of the pipe wall thickness. The pit clusters are randomly generated and superposed onto cosine tapers of depth 0 (no taper) 10, 20, 30, 40 and 50% of the pipe wall thickness, as indicated in the figure legend. In each case 100,000 randomly developed clusters were used in the calculations. The number of pit clusters resulting in maximum RCs larger

than approximately 8% is comparable regardless of cosine taper depth for all the cases investigated, which suggests that the cosine tapers have little effect on the largest maximum RCs in these cases, while the influence of the taper tends to increase the smallest RCs obtained. This is because large maximum RCs are generated by constructive interference between the pits in a cluster, while if there is destructive interference, the reflections from the individual pits cancel out, leaving just the effect of the taper. The shallower the taper, the more the maximum RCs approach the results found with pit cluster only; with cosine taper depth of 10%, only a slight deviation from the results with pit clusters without the cosine taper is seen. The figure inset highlights the 20% of the pit clusters resulting in the lowest maximum RCs, from which it can be seen, for example, that almost all pit clusters with maximum depth 60% of the pipe wall thickness with cosine taper depth of 30% or deeper give a maximum RC above 4%. Likewise, with a 20% deep cosine taper, approximately 2.5% of the pit clusters with maximum depth 60% result in a maximum RC below 3%, as is indicated by dashed lines in the figure inset.

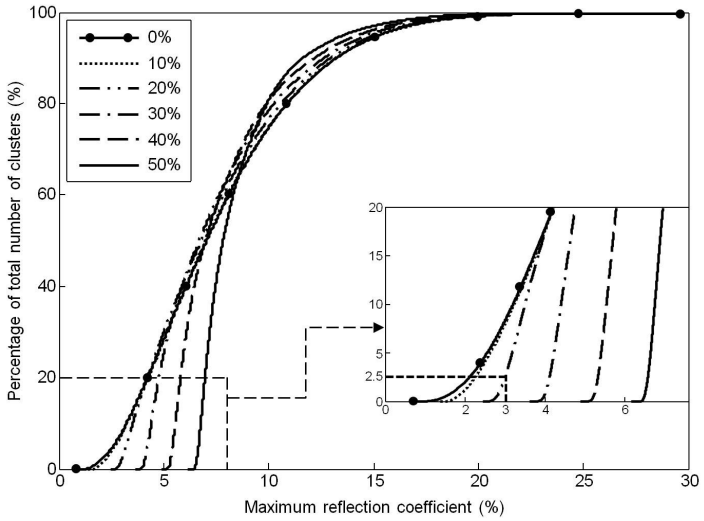

Figure 7: Percentage of clusters superposed onto a cosine taper of depth as indicated in the figure legend with a maximum RC that is less than the value of the abscissa for pit clusters with maximum defect depth deeper than, or equal to, 60% of the pipe wall thickness.

Thus, with realistic pit clusters, normally resulting in maximum RCs from 3-4% upwards, ultrasonic guided wave testing has been shown to have a high probability of detecting clusters before they penetrate through the wall thickness. Single, small and deep pits may not result in a sufficiently high RC to be detected at the low frequencies used in most practical guided wave testing. However, as pits typically tend to grow faster in width than in depth when they are in the millimetre scale [4, 5], commonly occur in clusters of multiple pits [4], and are part of a larger, broader attack [2], the detectability is good.

4 Summary

Initially, a parametric study of the reflection from two small circular holes at different relative positions in a pipe with the T(0,1) mode incident was reported. The reflection coefficient (RC) was found to be independent of the circumferential position of the holes and strongly dependent on their axial separation. The maximum RC was found to be comparable for all defect orientations. At separation distances shorter than 2*d*, where *d* is the defect diameter, multiple reflections between the defects increasingly influence the RC, which thus also was found to be the validity limit of superposition. With part-thickness defects, superposition was valid down to shorter separation distances as multiple scattering became less significant, which suggests that using superposition to simulate multiple part-depth defects and defect clusters will be satisfactory.

Employing the superposition technique, a study of the reflection of the fundamental torsional mode, T(0,1), from randomly generated pit clusters was then done. The maximum RC from pit clusters was found to be a linear function of the total volume fraction removed, but with very significant scatter due to interference between axially separated pits. Analyses indicated that most defect clusters with high maximum depth result in a maximum RC of 3-4% or higher

before they propagate fully through wall. Detailed analyses of typical problematic cases that gave small maximum RC values revealed that most of the clusters that resulted in small maximum RCs were due to single, small and deep defects in otherwise relatively shallow and lightly populated clusters. Despite such cluster morphologies being improbable in practice, some cases do occur and are likely to be missed by guided wave testing; in a few cases, destructive interference between pits in clusters consisting of several larger pits that were axially spaced relative to each other resulted in small maximum RCs.

More commonly pits are part of a larger, broader attack, with several pits of comparable depth in the pit cluster. Pit clusters superposed on cosine tapered defects were investigated to represent this case. With pit clusters being part of a larger attack, rather than growing in regions otherwise unaffected by corrosion, the cosine tapers alone were a lower bound for the maximum RC from the total cluster layouts; for example no pit clusters with maximum depth $\geq 60\%$ of the pipe wall thickness resulted in a maximum RC below 4% with cosine taper depth of 30% or deeper. This reduces the probability of deep defects not being detected. Thus, guided wave testing should preferably be carried out at multiple frequencies, and preferably regularly to monitor corrosion growth.

The main findings reported here were validated experimentally, as reported in [10] and [12].

Acknowledgements

This work has been carried out as part of my ph.d. thesis at Imperial College, London, UK, under the supervision of Prof. Peter Cawley. More elaborate discussions and results are published in refs. [10] and [12], as well as in [13].

References

[1] M. B. Kermani and A. Morshed, Carbon dioxide corrosion in oil and gas production – A compendium, *Corrosion*, 59 (8), 2003, 659-683.

[2] J. Kvarekvål, Morphology of localised corrosion attacks in sour environments, *Corrosion/2007*, paper 07659.

[3] A. Valor, F. Caleyo, L. Alfonso, D. Rivas and J. M. Hallen, Stochastic modelling of pitting corrosion: A new model for initiation and growth of multiple corrosion pits, *Corrosion science*, 49, 2007, 559-579.

[4] R. E. Melchers, Pitting corrosion of mild steel in marine immersion environment – Part 1: Maximum pit depth, *Corrosion*, 60, 2004, 24-36.

[5] G. Engelhart, H.-H. Strehblow, The determination of the shape of developing corrosion pits, *Corrosion science*, 1994, 36, 1711-25.

[6] R. Carandente, J. Ma and P. Cawley, The scattering of the fundamental torsional mode from axi-symmetric defects with varying depth profile in pipes, *J. Acoust. Soc Am.*, 127 (4), 2010, 3440-3448.

[7] A. Demma, P. Cawley, M. Lowe, A. G. Roosenbrand and B. Pavlakovic, The reflection of guided waves from notches in pipes: a guide for interpreting corrosion measurements, *NDT&E Int.*, 37, 2004, 167-180.

[8] F. B. Cegla, A. Rohde and M. Veidt, Analytical prediction and experimental measurement for mode conversion and scattering of plate waves at non-symmetric circular blind holes in isotropic plates, *Wave Motion*, 45, 2008, 162-177.

[9] A. Velichko and P. D. Wilcox, Excitation and scattering of guided waves: Relationships between solution for plates and pipes, *J. Acoust. Soc. Am.*, 125 (6), 2009, 3623-3631.

[10] A. Løvstad and P. Cawley, The reflection from the fundamental torsional mode from multiple circular holes in pipes, *NDT&E Int.*, 44, 2011, 553-562.

[11] P. J. Schafbuch, R. B. Thompson and F. J. Rizzo, Elastic scatterer interaction via generalized Born series and far-field approximations", *J. Acoust. Soc. Am.*, 93 (1), 1993, 295-307.

[12] A. Løvstad and P. Cawley, The reflection of the fundamental torsional mode from pit clusters in pipes, *NDT&E Int.*, 46, 2012, 83-93.

[13] A. Løvstad, *Detection of localised corrosion in pipes using guided waves*, ph.d. thesis, NTNU, 2012.